



Comparative Study for the Therapeutic Effect of Shark Care and 5-Fluorouracil Drugs in Mice with Hepatocellular Carcinoma in the Presence of Electric Field

**Rasha Said shams El Dine¹, Samir Ali Abd El-kaream², Soheir Mahmoud Elkholy¹,
Nadia Ahamed Abd El maniem³**

¹Medical Biophysics Department, Medical Research Institute, Alexandria University, Alexandria, Egypt

²Applied Medical Chemistry Department, Medical Research Institute, Alexandria University, Alexandria, Egypt

³Cancer Management and Research Department, Medical Research Institute, Alexandria University, Alexandria, Egypt

***Corresponding Author**

Rasha Said Shams El-Dine

Medical Biophysics Department

Medical research Institute

Alexandria University

Alexandria 2(03), Egypt

E-mail: Rasha_shams17@yahoo.com

Received: 11 April 2015; / Revised: 30 April 2015; / Accepted: 1 June 2015

Abstract

Hepatocellular carcinoma (HCC) is the third deadliest and fifth most common cancer worldwide. Many drugs that have the potential to treat cancers have had limited success due to their lack of efficient and safe delivery mechanisms that allow the drug molecules to cross cell membranes. Electrical pulses-mediated drug delivery, known as electroporation, is gaining attention as a possible approach to enhance uptake of chemotherapy. It delivers anticancer drugs with enhanced efficacy and fewer adverse effects. It is a physical (Thus, applicable to all types of tumors) and is minimally invasive. The aim of the present work was to compare the therapeutic effect of shark care and 5-Fluorouracil drugs in mice with HCC in the presence of electric field. The present study was conducted on 50 albino mice weighting 20-25 gm of 8-10 weeks of age were divided into gp (A) (control), gp (B-1), (That donot recive any treatment), gp (B-2) (which treated by injected by 120 mg/kg of 5-Fluorouracil), gp (B-3) (which treated by shark care drug dissolved in drinking water daily). And after this treatment period part of gp (B-2-i), gp (B-3-i) don't exposed to electric field while gp (B-2 -ii) and gp (B-3-ii) were exposed to electric field for 5 second and the last part gp (B-2-iii) and gp (B-3-iii) were exposed to electric field for 10 second. Parts of liver tissue and blood samples were collected from all from mice of each group for histopathological examination, biophysical study (Capacitance and resistance were measured using LCR meter over a frequency range from 1-100KHz and the measured values were used to calculate permittivity and conductivity) and biochemical study (molecular detection of Alpha-fetoprotein (AFP) and transforming growth factor beta-1(TGβ1) mRNAs by RT-PCR) before and after treatment by shark care and 5-Fluorouracil drugs in mice with HCC in the presence of

electric field. During the whole course of experiment the histopathological changes were synchronized with the biophysical (permittivity and conductivity) and biochemical (AFP and TG β 1 mRNAs gene expression) changes. shark care drug showed promising effective results for treatment of HCC compared to results obtained with 5-Fluorouracil drug. presence of electric field results in reduced tumor growth, and induction of apoptosis in the treated cells by enhancing uptake of chemotherapy and delivering anticancer drugs with enhanced efficacy and fewer adverse effects.

Keywords: 5-Fluorouracil, shark care AFP-mRNA, TG β 1 mRNA, DAB, HCC.

1. Introduction

Liver cancer rapidly reduces quality of life and typically causes death 6 months : 1 year from diagnosis.⁽¹⁾ Globally, it is the fifth in cancer incidence and the third leading cause of cancer death.^(1,2) In Egypt, between 1993 and 2003, there was an almost two fold increases from about 4% in 1993 to 7.3 % in 2003) in HCC among patients with chronic liver diseases.⁽³⁻⁶⁾ Egypt is now plagued by the highest prevalence of HCC in the world, which ranged from 6 to 28% and a reported average of about 13.8%.^(7,8) Recent investigations in Egypt have also shown the increasing importance of HCV infection in the aetiology of HCC, which now estimated to account for 40-50% of cases.⁽⁴⁻⁶⁾

The best characterized agents of chemotherapeutic drugs for the treatment of HCC are the halogenated pyrimidines, a group that includes fluorouracil (5-fluorouracil or 5-Fu). Or floxuridine (5-fluoro 2 deoxyuridine, or 5- FudR) and idoxuridine (5-iododeoxy uridine).⁽⁹⁾

The treatment by new specific antiangiogenic drug and monitoring such treatment need reliable standardized and useful predicative markers of antiangiogenesis.⁽¹⁰⁾ Such biomarker must be easily measurable, reflecting accurately the pathological process that it is designed to measure and must provide the clinician with an answer that can be easily interpreted.⁽¹¹⁾

Shark care drug is a purified Shark cartilage extract composed of the following ingredients: proteins: (Collagen, U-995 protein and SCF2 protein), glycosaminoglycans: (Chondroitin-6-sulfate and keratin sulphate) and calcium salts.⁽¹²⁾

Many drugs that have the potential to treat cancers have had limited success due to their lack

of efficient and safe delivery mechanisms that allow the drug molecules to cross cell membranes. Electrical pulses-mediated drug delivery, known as electroporation, is gaining attention as a possible approach to enhance uptake of chemotherapy. It delivers anticancer drugs with enhanced efficacy and fewer adverse effects. It is a physical (Thus, applicable to all types of tumors) and is minimally invasive.

The aim of the present work was to compare the therapeutic effect of shark care and 5-Fluorouracil drugs in mice with HCC in the presence of electric field.

The study was done on fifty albino mice weighting 20-25 gm of 8-10 weeks of age were divided into four groups.

Group A: 10 mice were used as a control group, **group B:** 40 mice have induced HCC by DABE this group were subdivided into three sub-groups; sub group B - 1: 10 mice which were not received any treatment, and were kept at room environment and were exposed to (LG1100) MCP corp, sub group B - 2: 15 mice were injected intraperitoneal with 120 mg/kg body weight of 5-Fluorouracil dose every day for 21days and divided into (sub group B - 2i : 5 mice were sacrificed for histopathological after 21 days, sub group B - 2ii: 5 mice were exposed to (LG1100) MCP corp for 5 sec after 21 days, sub group B - 2iii:5 mice were exposed to (LG1100) MCP corp for 10 sec after 21 days) and sub group B - 3: 15 mice were treated by shark care drug dissolved in drinking water daily for 21 days and divided into (sub group B – 3 i:5 mice were sacrificed and histopathological after 21 days, sub group B – 3 ii:5 mice were exposed to (LG1100) MCP corp for 5 sec after 21 days, sub group B – 3 iii:5 mice were

exposed to (LG1100) MCP corp for 10 sec after 21 days)

2. Histopathological Examination

Parts of liver tissue from mice of each previous groups were processed and examined by Hematoxylin and Eosin (H&E).⁽¹³⁾

3. Biophysical Examination

3.1 Measuring electrodes

Each sample was connected to the LCR meter (Instek Model 819, Japan) by means of two silver-silver chloride electrodes. Specimens were inserted in contact between the two electrodes. The electrodes were held in position during the measurements by means of gallows like stand, the gallows used only for convenience in supporting the movable electrode. Sliver chloride electrodes provided a good contact within minimum polarization and compatibility with biological cells. The contact to the specimen was through KCL gel.

3.2 Measurements

Capacitance C and resistance R was measured using LCR meter (Good will instrument Co. Ltd, Hsien Taiwan) over a frequency range from 1-100KHz. The measured values were used to calculate permittivity and conductivity.

The relative dielectric permittivity and conductivity were calculated from the equation:⁽¹⁴⁾

$$C = \epsilon' \epsilon_0 A / d \quad (1)$$

$$G = \sigma A / d \quad (2)$$

Where C and G were the capacitance and conductance of the capacitor between the two measuring electrodes in (Farad) and in (Siemens), respectively, A was the surface area of the electrode in (m²), d was the separation between the two electrodes in (m), ϵ' was the relative permittivity in (farad/meter), ϵ_0 was the permittivity of vacum (8.85×10^{-12} F/m) and σ was the electrical conductivity in (Siemens/ m)

The imaginary parts of complex permeittivity ϵ'' and conductivity σ'' were calculated according to the relation.^(15,16)

$$\epsilon'' = (\sigma - \sigma_L) / 2 \pi f_2 \epsilon_0 \quad (3)$$

$$\sigma'' = 2 \pi f_2 \epsilon_0 (\epsilon - \epsilon_h) \quad (4)$$

Where: σ_L was the low frequency limiting conductivity taken at 1 KHz ϵ_h was the high frequency limiting permittivity taken at 100 KHZ.

4. Biochemical Examination

4.1 RT-PCR for AFP- mRNA and TG β 1- mRNA genes expression amplification

4.1.1 RNA extraction:

RNA was extracted from the serum of mice using QIAamp RNA blood mini kit, was purchased from QIAGEN, USA according to the manufacturer's instructions.

Preparation of Full-Length First strand cDNA from RNA template using RevertAidTM First Strand cDNA Synthesis Kit.⁽¹⁷⁾

4.1.2 Reverse transcription

Reverse transcription reaction was carried out in a 20 μ l reaction mixture by using RevertAidTM First Strand cDNA Synthesis Kit Cdna Synthesis Kit# K1621,#1622, was purchased from MBI Fermentas, Lithuania according to manufacture's instruction.

4.1.3 RT-PCR amplification

To each PCR tube the following were added 5 μ l (0.25 μ g) Template AFP- cDNA, 10 μ l2 TaqTM Green PCR Master Mix (2X) {dNTPs [0.4 mM of each dATP, dCTP, dGTP, dTTP], 0.05u/ μ l Taq DNA polymerase and reaction buffer} # k1081, was purchased from MBI Fermentas, Lithuania, 1.5 μ l AFP forward primer: 5' - TGAGCTTCCTGCATTGGGAG - 3', 1.5 μ l AFP reverse primers: 5' - CCCGCCAGCATCATAGCTTA - 3' and deionized-RNase free water to final volume 20 μ l. The reaction mixtures were gently vortexed, briefly centrifuged to collection all drops to the bottom of the tubes, then were placed in the

thermal cycler (Little Genius, Bioer Co), The PCR mixture was subjected to 35 amplification cycles. PCR conditions were as follows: An initial denaturation (94°C, 2min), followed by 35 cycles of denaturation (94°C, 1min), annealing (52°C, 1min), and extension (72°C, 1min), with a final extension (72°C, 7min).

To each PCR tube the following were added 5 µl (0.25 µg) Template TGβ1- cDNA, 10 µl 2 X PCR Master Mix {dNTPs [0.4 mM of each dATP, dCTP, dGTP, dTTP], 0.05u/µl Taq DNA polymerase and reaction buffer}, 1.5 µl AFP forward primer: 5' - GTCCTGGCCTTAGCTGTCTT- 3', 1.5 µl AFP reverse primers: 5' - ATTCCATAGGCCTGTGACGC- 3' and deionized-RNase free water to final volume 20 µl. The reaction mixtures were gently vortexed, briefly centrifuged to collection all drops to the bottom of the tubes, then were placed in the thermal cycler (Little Genius, Bioer Co), The PCR mixture was subjected to 35 amplification cycles. PCR conditions were as follows: An initial denaturation (94°C, 2min), followed by 35 cycles of denaturation (94°C, 1min), annealing (52°C, 1min), and extension (72°C, 1min), with a final extension (72°C, 7min).

To verify the successful preparation of mRNA and as positive controls, samples were detected for the presence of glyceraldehyde-3-phosphate dehydrogenase (GAPDH) mRNA. forward primer: 5' - AGGCCGGTGCTGAGTATGTC - 3', reverse primers: 5' - TGCCTGCTTACCACCTTCT - 3'. Reaction tubes containing no cDNA control template and without cDNA sample addition were included as negative controls for each PCR reaction.

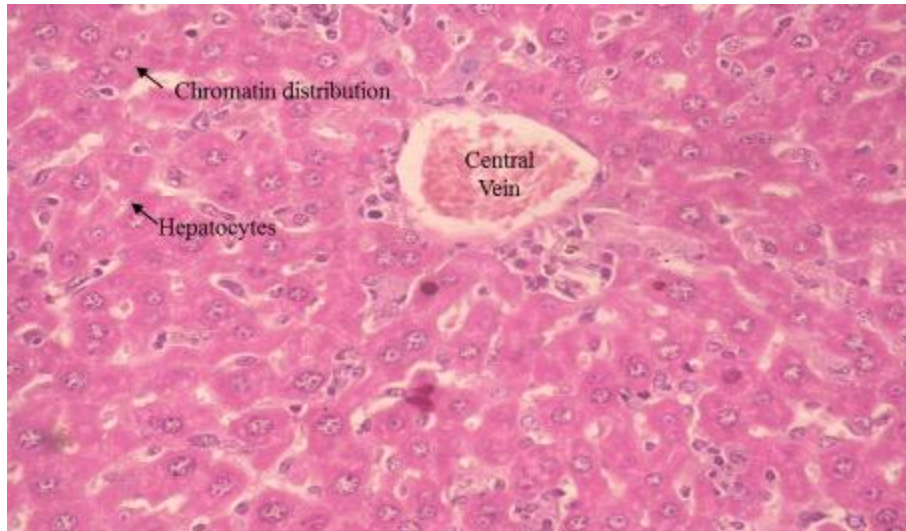
4.2 Detection

The amplicons were analyzed with 2% (wt/vol) ethidium bromide stained agarose gel.

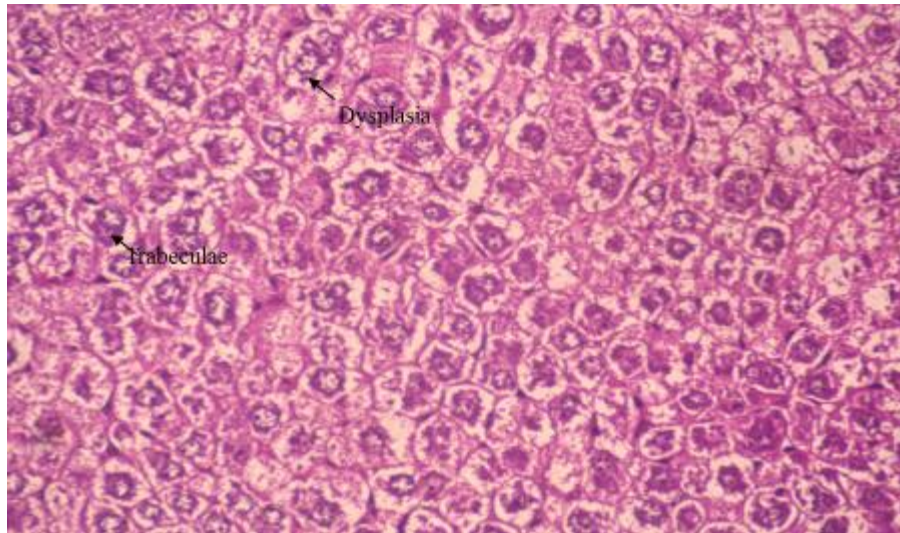
The bands were visualized on a 302 nm UV transilluminator (BIO-RAD, USA). The gel was examined for bands of 294bp as determined by the molecular weight marker (Gene Ruler™ 100bp plus DNA Ladder, ready-to-use#SM0323, was purchased from Fermentas, Lithuania) runs at the same time and then photographed using digital camera (SONY Super Steady Shot DSC-W300).

5. Results

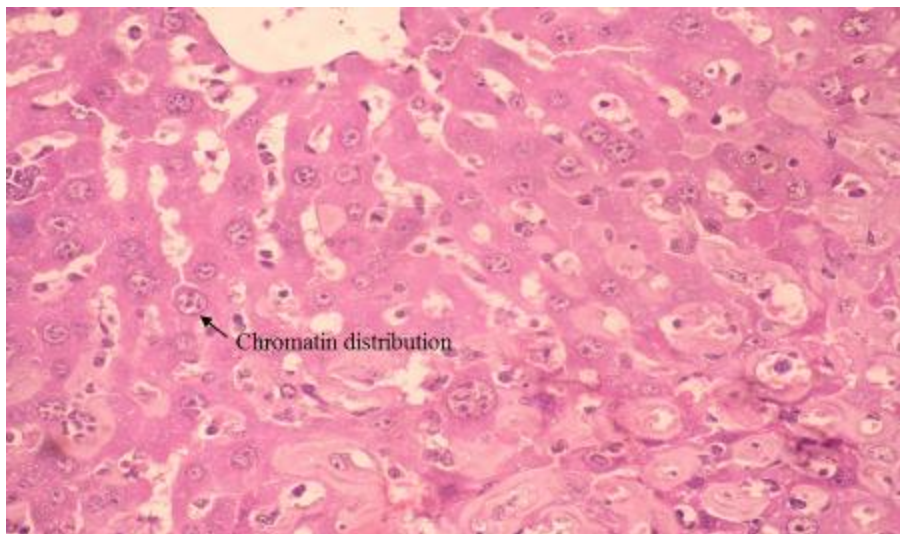
In the present work Histological examination was performed on all study groups and Coded H and E stained slides were examined microscopically by a single pathologist using a high power (magnification, ×400), and at least five high-power fields were examined to detect histopathological changes: gp (A) (control); showed 1- normal hepatic architecture, gp (B-1), (That donot recive any treatment); showed less preserved hepatic architecture with focal cytoplasmic vaculation of hepatocyte, mild fibrosis and lymphatic infiltration 2- vascular degeneration and ballooning of hepatocyte with moderate fibrosis 3- areas of coagulative necrosis 4- various degree of dysplasia and finally HCC, gp (B-2) (which treated by injected by 120 mg/kg of 5-Fluorouracil); showed moderate lymphatic infiltration also moderate necrosis and moderate nuclear displeases (nuclear elnargment prominent nuclei), gp (B-3) (which treated by shark care drug dissolved in drinking water daily); showed showed mild lymphatic infiltration also mild necrosis and mild nuclear displeases (nuclear elnargment prominent nuclei), gp (B-2-ii) and gp (B-3-ii) were exposed to electric field for 5 second and the last part gp (B-2-iii) and gp (B-3-iii) were exposed to electric field for 10 second; showed no fibrosis and no necrosis with relative chromatin distribution and relatively normal hepatocyte.



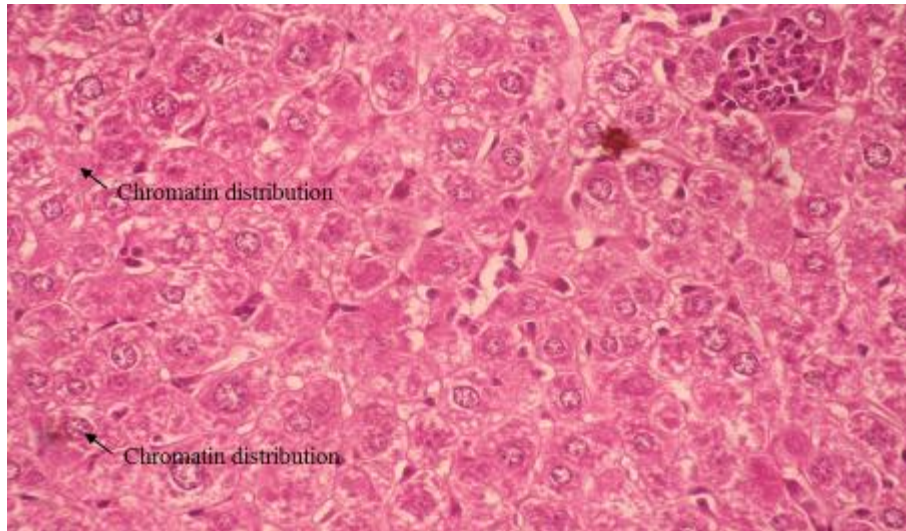
Figure(1): The group of control normal hepatocytes showing no dysplasia.



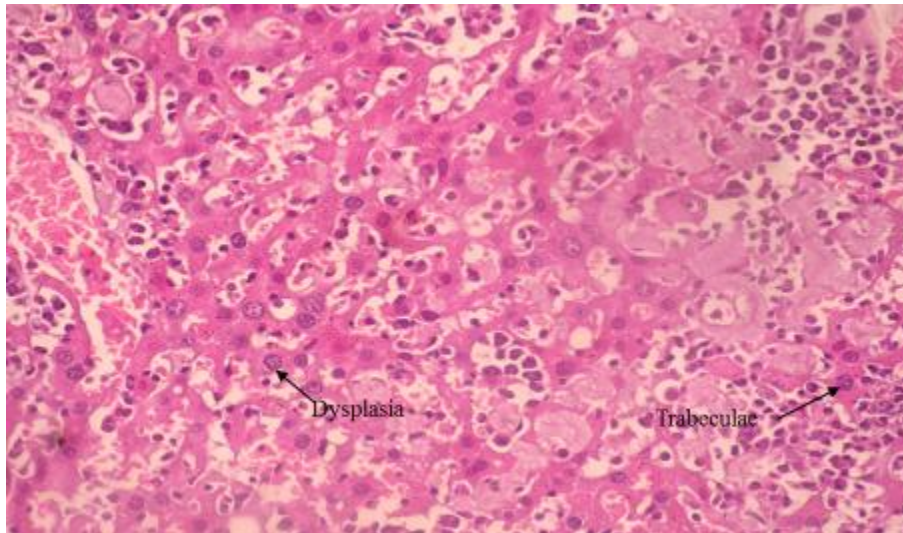
Figure(2): The groups that have HCC.



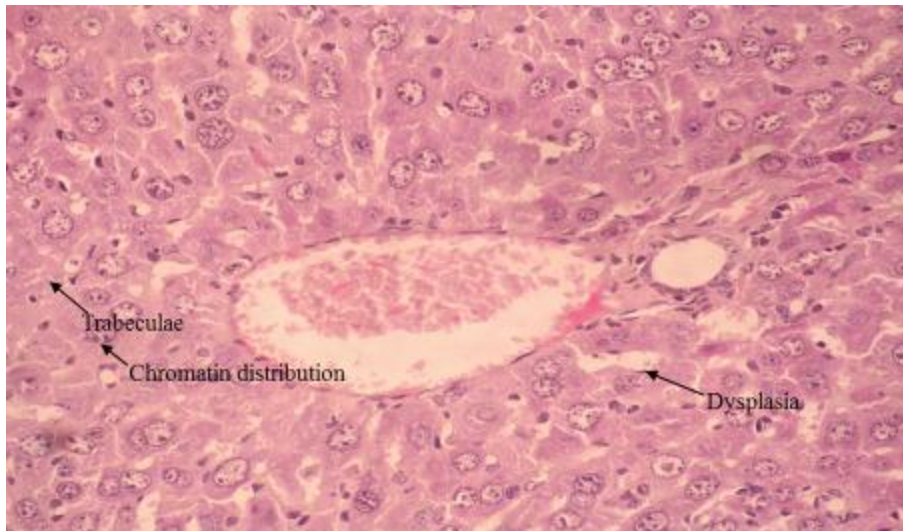
Figure(3): The group of 5- Fluorouracil after 21 days and exposed to electric field for 5 sec reveals change in pattern of chromatin distribution .



Figure(4): The group of 5- Fluorouracil after 21 days exposed to electric field for 10 sec reveals change in pattern of chromatin distribution



Figure(5): The group of Shark care after 21 days exposed to electric field for 5 sec reveals in pattern of chromatin distribution.



Figure(6): The group of Shark care after 21 days exposed to electric field for 10 sec reveals change in pattern of chromatin distribution.

i - Dielectric parameters of mice s liver tissue.

a- Effects of different doses of 5- fluorouracil a shark care on permittivity and conductivity variation with frequency.

Figures (7-16) show set of the measured permittivity, and conductivity with the frequency of mice liver tissues of gp (A) (control), gp (B-2) (which treated by injected by 120 mg/kg of 5-Fluorouracil) and gp (B-3) (which treated by shark care drug dissolved in drinking water daily). Generally, the permittivity decrease, while the real conductivity increases with increasing of frequency.

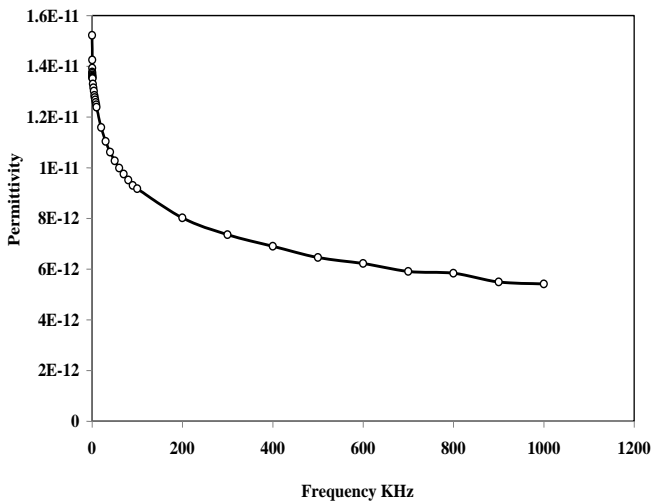


Figure (7): Variation of permittivity with frequency for mice liver tissues Control.

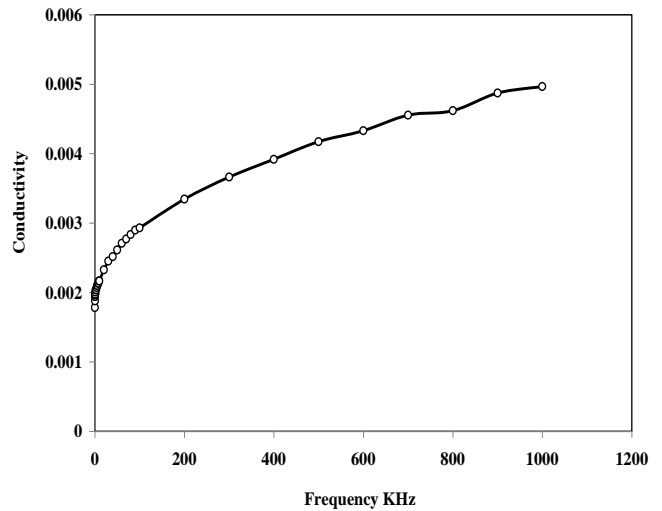


Figure (8): Variation of Conductivity with frequency for mice liver tissues Control.

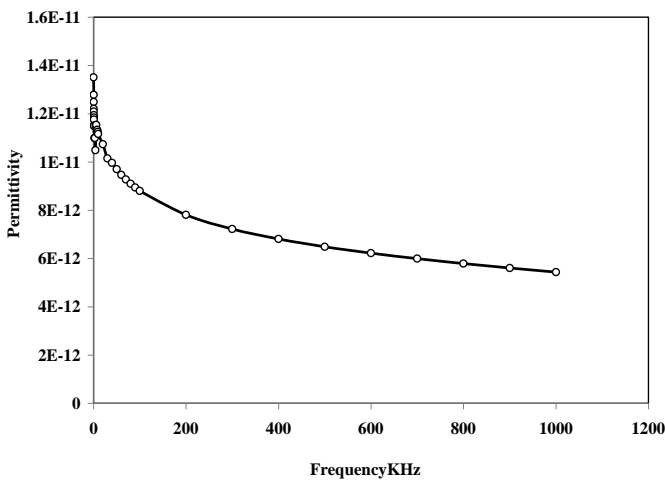


Figure (9): Variation of permittivity with frequency of mice liver tissues treated by injected by 120 mg/kg of 5-Fluorouracil after exposed to electric field for 5 sec.

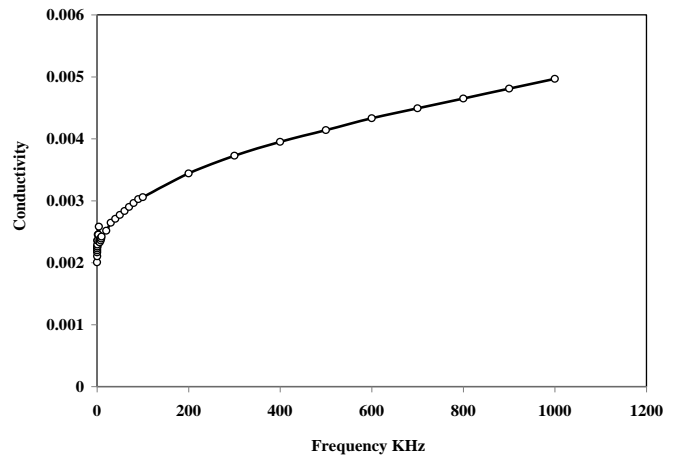


Figure (10): Variation of conductivity with frequency of mice liver tissues treated by injected by 120 mg/kg of 5-Fluorouracil after exposed to electric field for 5 sec.

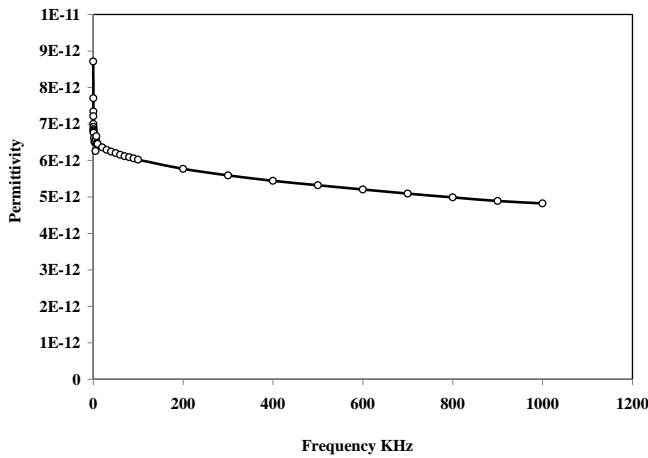


Figure (11): Variation of permittivity with frequency of mice liver tissues treated by injected by 120 mg/kg of 5-Fluorouracil after exposed to electric field for 10 sec.

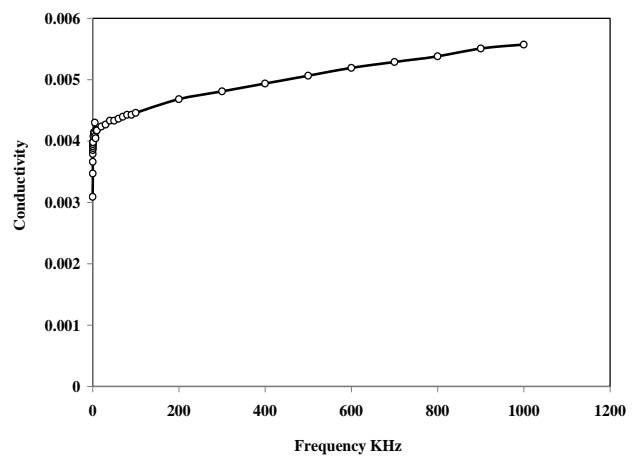


Figure (12): Variation of conductivity with frequency of mice liver tissues treated by injected by 120 mg/kg of 5-Fluorouracil after exposed to electric field for 10 sec.

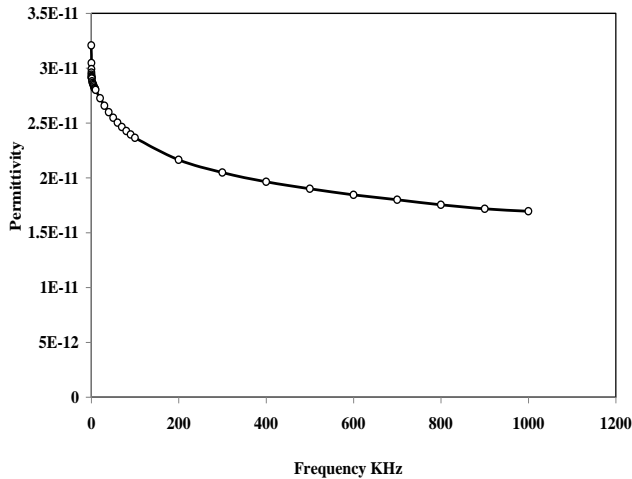


Figure (13): Variation of permittivity with frequency of mice liver tissues treated by shark care drug dissolved in drinking water daily after exposed to electric field for 5sec.

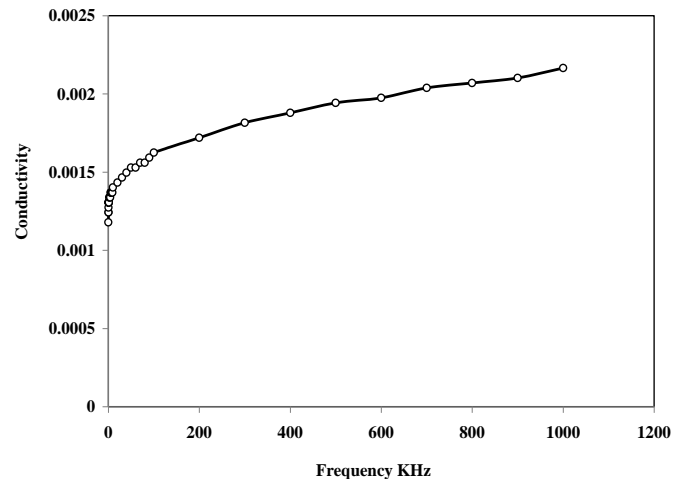


Figure (14): Variation of conductivity with frequency of mice liver tissues treated by shark care drug dissolved in drinking water daily after exposed to electric field for 5sec.

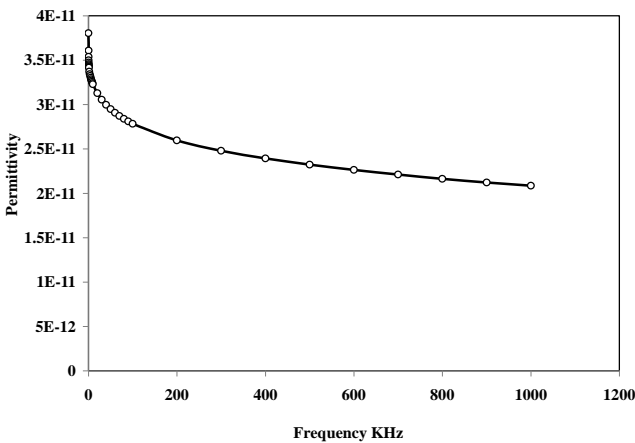


Figure (15): Variation of permittivity with frequency of mice liver tissues treated by shark care drug dissolved in drinking water daily after exposed to electric field for 10 sec.

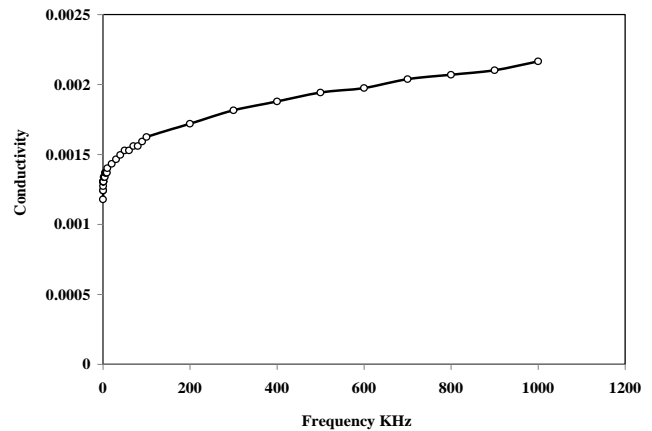


Figure (16): Variation of conductivity with frequency of mice liver tissues treated by shark care drug dissolved in drinking water daily after exposed to electric field for 10 sec.

b- Complex permittivity and conductivity diagrams

Figures (17-18), Illustrate the diagrams of complex permittivity and conductivity of liver tissues of gp (A) (control), gp (B-1), (That donot recive any treatment), gp (B-2) (which treated by injected by 120 mg/kg of 5-Fluorouracil), gp (B-3) (which treated by shark care drug dissolved in drinking water daily). And after this treatment period part of gp (B-2-i), gp (B-3-i) Which exposed to electric field for 5 second while gp (B-2 -ii) and gp (B-3-ii) were exposed to electric field for 10 second. As seen in these diagrams the depree of depressed center and the maximum values of the real and imaginary permittivity and conductivity depend on the dose of paraqat used.

The Complex permittivity diagram Figure (17), follow the Cole-Cole semi circle pattern except at low frequency due to cell polarization. The maximum permittivity peaks corresponding to groups treated by injected by 120 mg/kg of 5-Fluorouracil after exposed to electric field for 5 sec,

groups that treated by same dose of 5-Fluorouracil but exposed to electric field for 10 sec, groups tissues treated by shark care drug dissolved in drinking water daily after exposed to electric field for 5sec, and groups treated by shark care drug dissolved in drinking water daily after exposed to electric field for 10sec are lower and have a small reative distance of base decrement than that of control group. i.e., The semi circle radii of gp (B-2-i) (group that treated by injected by 120 mg/kg of 5-Fluorouracil after exposed to electric field for 5 sec), gp (B-3-i) (group that treated by shark care drug dissolved in drinking water daily after exposed to electric field for 5 sec), gp (B-2 -ii) (group that treated by injected by 120 mg/kg of 5-Fluorouracil after exposed to electric field for 10 sec) and gp (B-3-ii) (group that treated by shark care drug dissolved in drinking water daily after exposed to electric field for 10 sec).are smaller than that of the gp (A) (control) .

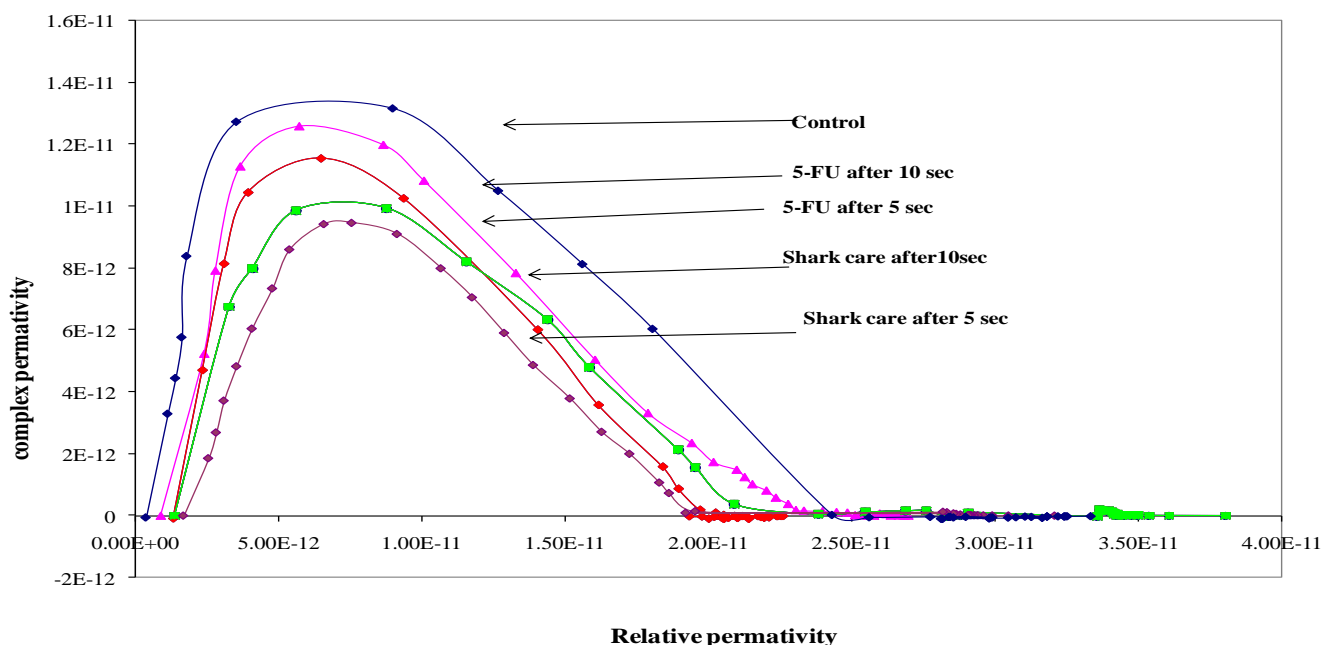


Figure (17): The Complex permittivity diagram

The complex conductivity diagram Figure (18), follows the Cole – Cole semi circle pattern. The diagrams of gp (B-2-i) (group that treated by injected by 120 mg/kg of 5-Fluorouracil after

exposed to electric field for 5 sec), gp (B-2 -ii) (group that treated by injected by 120 mg/kg of 5-Fluorouracil after exposed to electric field for 10 sec) are fare away than the control compared to the

groups of gp (B-3-i) (group that treated by shark care drug dissolved in drinking water daily after exposed to electric field for 5 sec), and gp (B-3-ii) (group that treated by shark care drug dissolved in

drinking water daily after exposed to electric field for 10 sec). Which are nerarest to the gp (A) (control) .

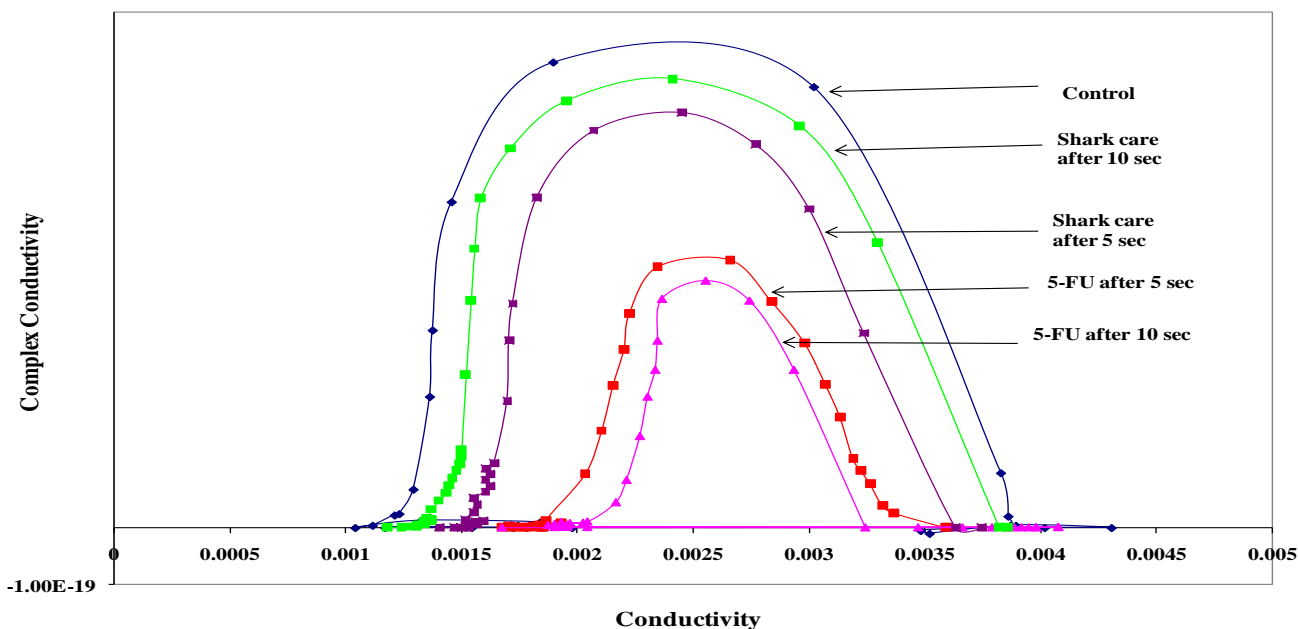


Figure (18): The complex conductivity diagram.

In the present study molecular study of AFP and TGF- β 1 gene expression as a molecular diagnostic and prognostic markers for HCC revealed a significant increase in the expression of AFP-mRNA and TGF- β 1-mRNA genes at sub group B1 after administration of DAB as compared to group A, at the same time histopathological changes were also seen.

Sub group B3ii showed a relatively lower genes expression of AFP-mRNA and TGF- β 1-mRNA than B2ii and these reduction had its impact on the histopathological findings. This results indicated that treatment with shark care showed promising way for treatment of HCC than traditional chemotherapeutic 5-fluorouracil.

Sub group B3iii showed much lower genes expression of AFP-mRNA and TGF- β 1-mRNA than B2iii and these reduction had its impact on the histopathological findings. This results revealed that electrical pulses-mediated drug delivery is

gaining attention as a possible approach to enhance uptake of chemotherapy.

The data in the present study showed that during the whole course of experiment the histopathological changes were synchronized with the biochemical changes. Molecular detection of AFP-mRNA and TGF- β 1-mRNA genes expression using RT-PCR could be used as a diagnostic and prognostic predictor of HC

6. Discussion

The application of pulsed fields has emerged as a local non-thermal and druge-free therapy for cancer. Pulsed electric field (PEF) therapy is a procedure using intense but short electric pulses that provoke either permanent permeabilization of cancer cells or destabilize the cell membranes and inteacellular components to which the cells are unable to repair resulting in their death.⁽¹⁷⁾

Amplification of mRNA-AFP gene by RT-PCR:

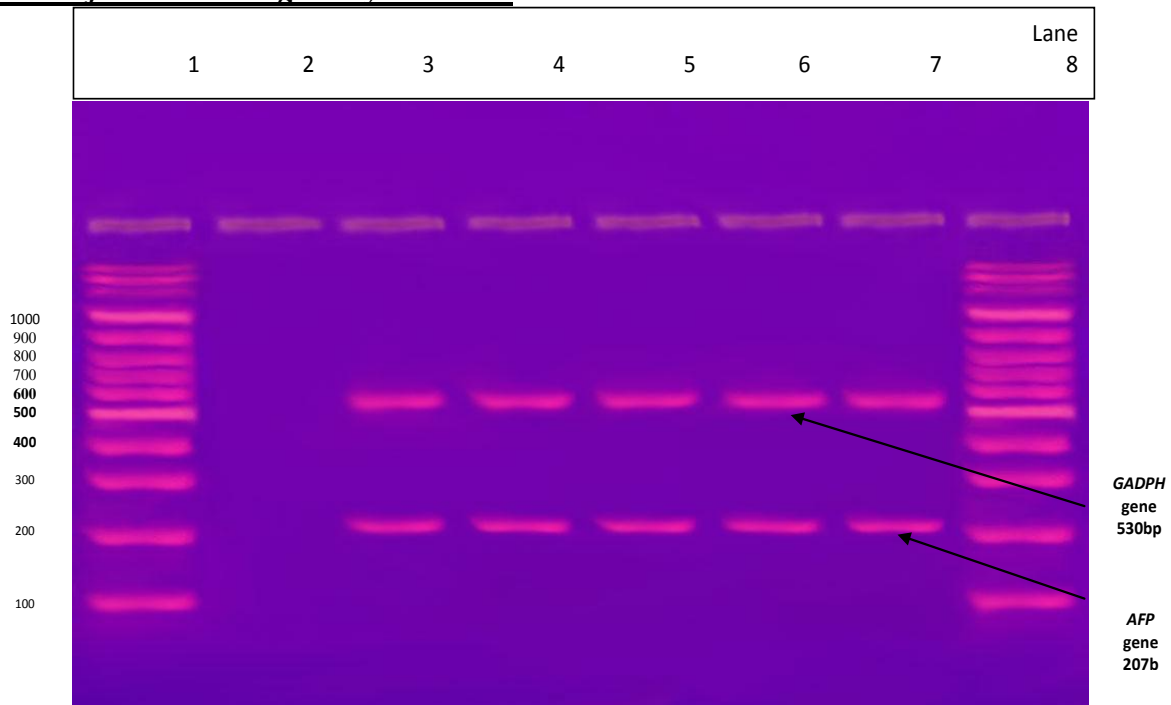


Figure (19): Ethidium bromide stained agarose gel showing bands of amplified PCR products of *mRNA-AFP* gene of Sub group B – 2i: 5 mice were injected intraperitoneal with 120 mg/kg body weight of 5-Fluorouracil dose every day for 21 days blood samples: Lane 1 and 8 marked the DNA marker, Lane 2 showing negative control (DNA nuclease free water), , lane 3- 7 marked positive cases showing amplified bands of 207 bp. (530 bp representing *GADPH* gene as positive control).

Amplification of mRNA-AFP gene by RT-PCR:

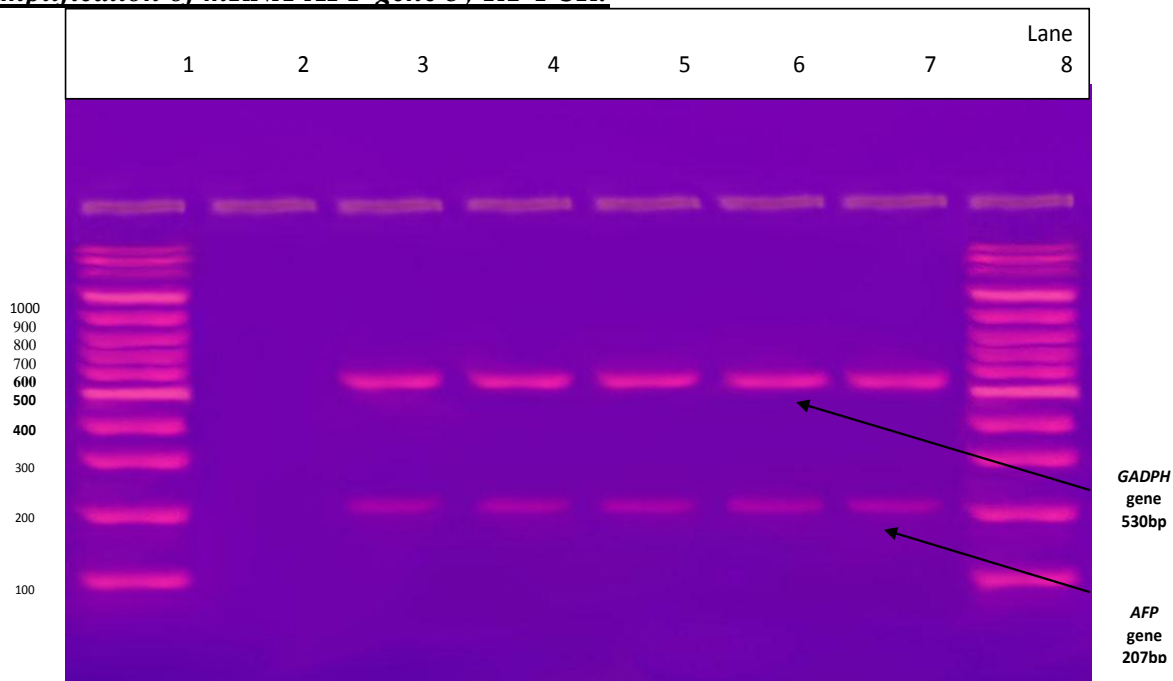


Figure (20): Ethidium bromide stained agarose gel showing bands of amplified PCR products of *mRNA-AFP* gene of Sub group B – 2ii: 5 mice were injected intraperitoneal with 120 mg/kg body weight of 5-Fluorouracil dose every day for 21 days and were exposed to(LG1100) MCP corp for 5 sec blood samples: Lane 1 and 8 marked the DNA marker, Lane 2 showing negative control (DNA nuclease free water), , lane 3- 7 marked positive cases showing amplified bands of 207 bp. (530 bp representing *GADPH* gene as positive control).

Amplification of mRNA-AFP gene by RT-PCR:

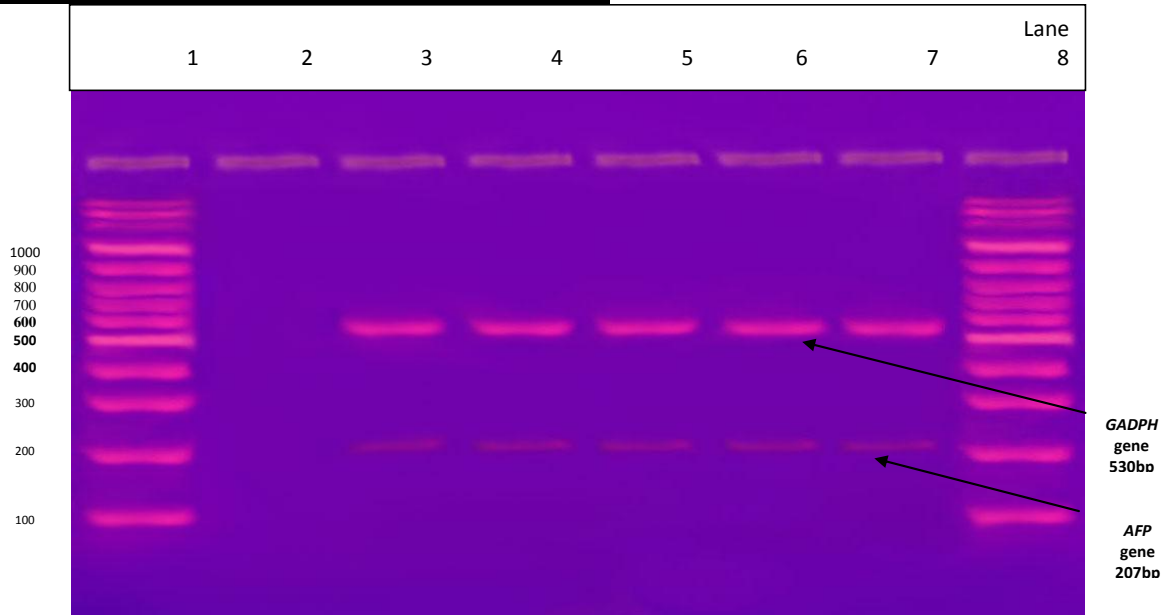


Figure (21): Ethidium bromide stained agarose gel showing bands of amplified PCR products of *mRNA-AFP* gene of Sub group B – 2iii: 5 mice were injected intraperitoneal with 120 mg/kg body weight of 5-Fluorouracil dose every day for 21 days and were exposed to(LG1100) MCP corp for 10 sec blood samples: Lane 1 and 8 marked the DNA marker, Lane 2 showing negative control (DNA nuclease free water), , lane 3- 7 marked positive cases showing amplified bands of 207 bp. (530 bp representing *GADPH* gene as positive control).

Amplification of mRNA-AFP gene by RT-PCR:

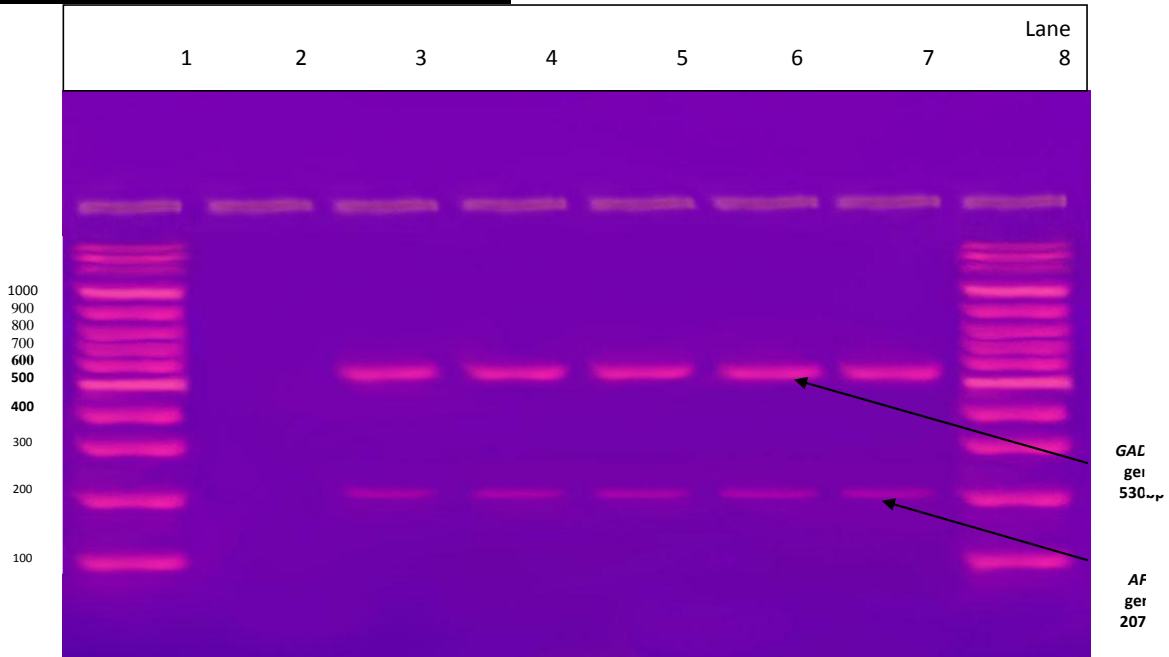


Figure (22): Ethidium bromide stained agarose gel showing bands of amplified PCR products of *mRNA-AFP* gene of Sub of group B – 3ii: 5 mice were treated by shark care drug dissolved in drinking water daily for 21 days and were exposed to(LG1100) MCP corp for 5 sec blood samples: Lane 1 and 8 marked the DNA marker, Lane 2 showing negative control (DNA nuclease free water), , lane 3- 7 marked positive cases showing amplified bands of 207 bp. (530 bp representing *GADPH* gene as positive control).

Amplification of mRNA-AFP gene by RT-PCR:

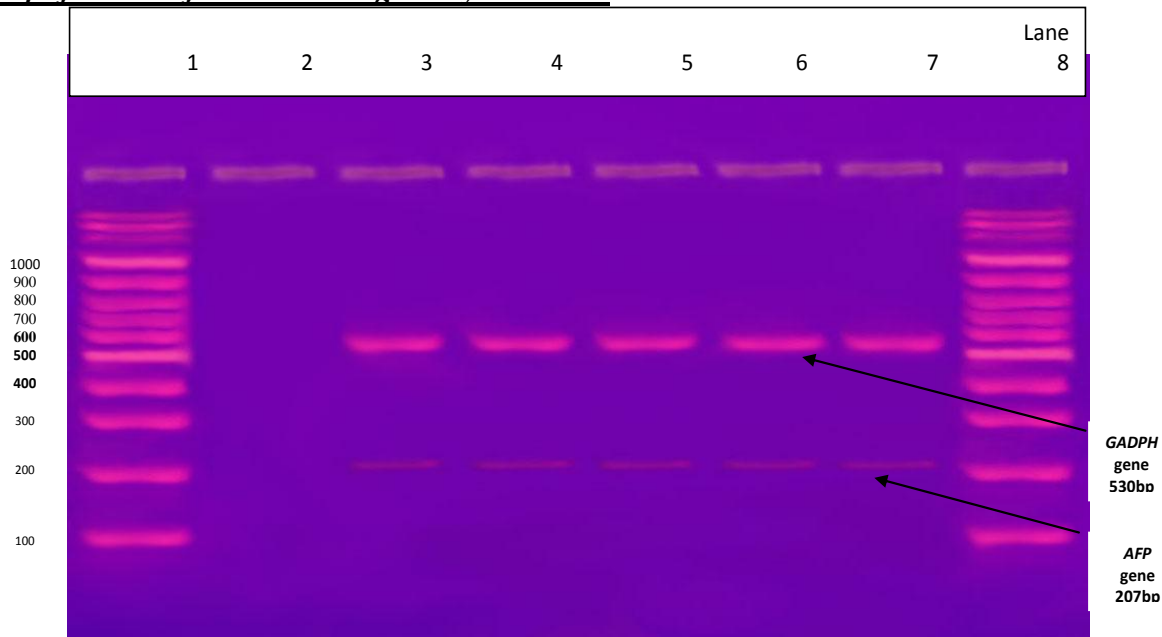


Figure (23): Ethidium bromide stained agarose gel showing bands of amplified PCR products of *mRNA-AFP* gene of Sub of group B – 3iii: 5 mice were treated by shark care drug dissolved in drinking water daily for 21 days and were exposed to(LG1100) MCP corp for 10 sec blood samples: Lane 1 and 8 marked the DNA marker, Lane 2 showing negative control (DNA nuclease free water), , lane 3- 7 marked positive cases showing amplified bands of 207 bp. (530 bp representing *GADPH* gene as positive control).

Amplification of mRNA-TGFβ1 gene by RT-PCR:

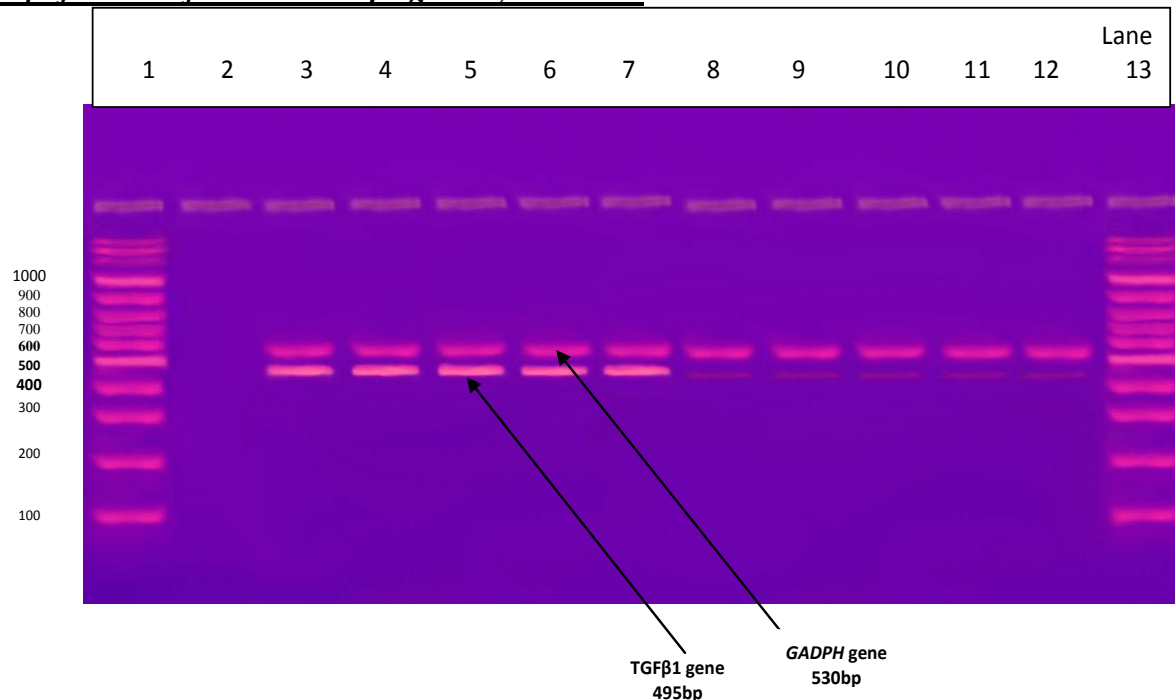


Figure (24): Ethidium bromide stained agarose gel showing bands of amplified PCR products of *mRNA-TGFβ1* gene of Sub group B -1; mice have induced HCC by DABE and have not received any treatment blood samples: Lane 1 and 13 marked the DNA marker, Lane 2 showing negative control (DNA nuclease free water), lane 3- 7 marked positive cases showing amplified bands of 495 bp and lane 8- 12 marked positive cases of control group mice (530 bp representing *GADPH* gene as positive control).

Amplification of mRNA- TGFβ1 gene by RT-PCR:

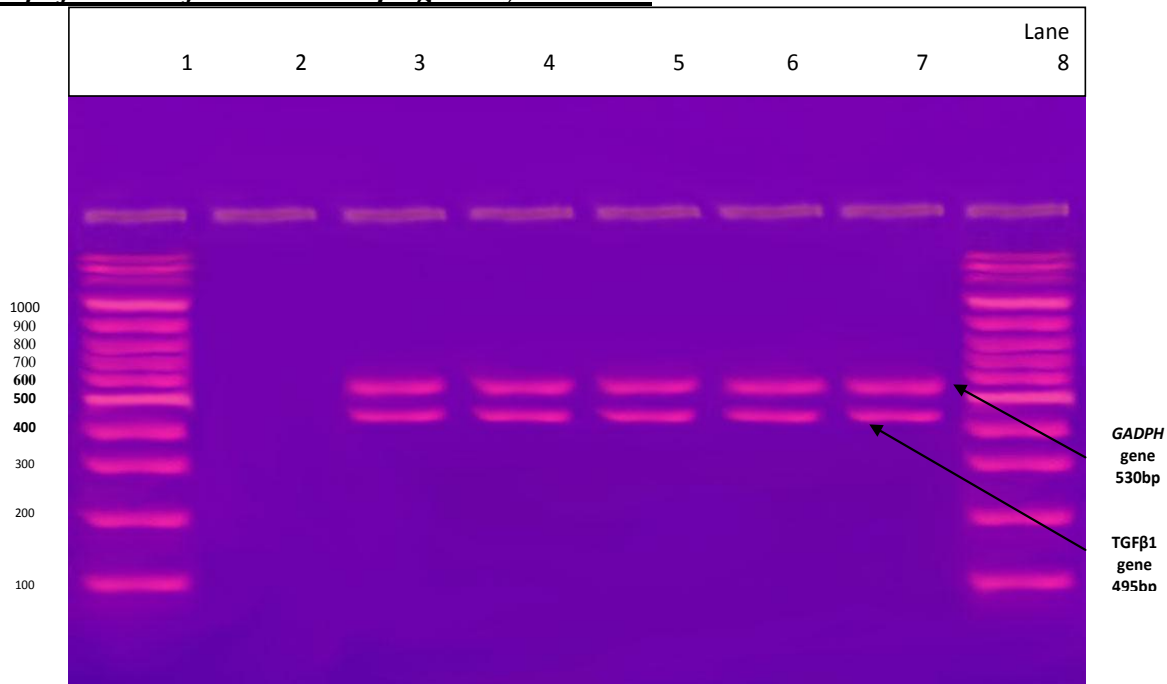


Figure (25): Ethidium bromide stained agarose gel showing bands of amplified PCR products of *mRNA- TGFβ1* gene of Sub group B – 2i: 5 mice were injected intraperitoneal with 120 mg/kg body weight of 5-Fluorouracil dose every day for 21 days blood samples: Lane 1 and 8 marked the DNA marker, Lane 2 showing negative control (DNA nuclease free water), , lane 3- 7 marked positive cases showing amplified bands of 495 bp. (530 bp representing *GADPH* gene as positive control).

Amplification of mRNA- TGFβ1 gene by RT-PCR:

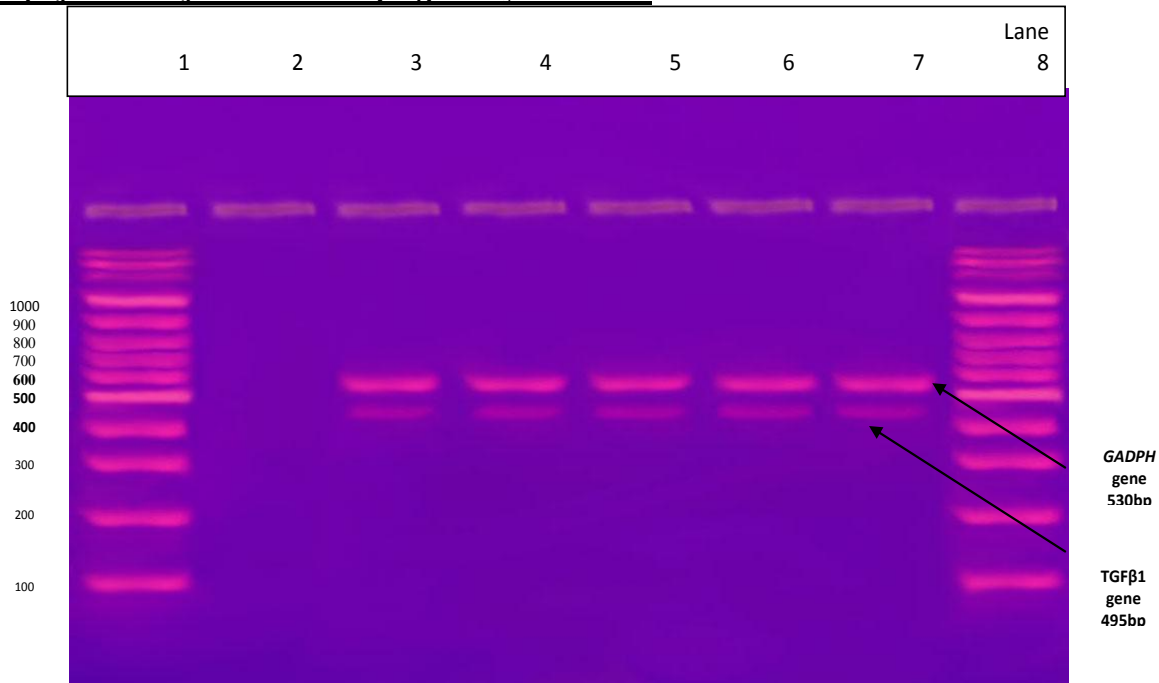


Figure (26): Ethidium bromide stained agarose gel showing bands of amplified PCR products of *mRNA- TGFβ1* gene of Sub group B – 2ii: 5 mice were injected intraperitoneal with 120 mg/kg body weight of 5-Fluorouracil dose every day for 21 days and were exposed to (LG1100) MCP corp for 5 sec blood samples: Lane 1 and 8 marked the DNA marker, Lane 2 showing negative control (DNA nuclease free water), , lane 3- 7 marked positive cases showing amplified bands of 495 bp. (530 bp representing *GADPH* gene as positive control).

Amplification of mRNA- TGFβ1 gene by RT-PCR:

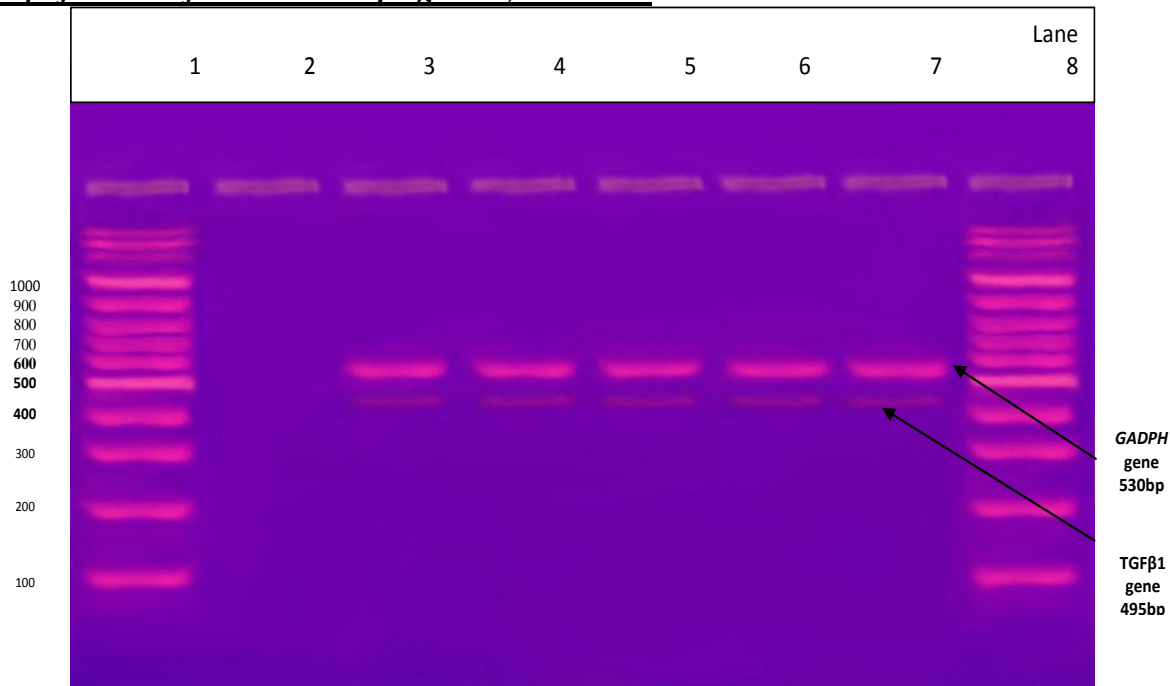


Figure (27): Ethidium bromide stained agarose gel showing bands of amplified PCR products of *mRNA- TGFβ1* gene of Sub group B – 2iii: 5 mice were injected intraperitoneal with 120 mg/kg body weight of 5-Fluorouracil dose every day for 21 days and were exposed to(LG1100) MCP corp for 10 sec blood samples: Lane 1 and 8 marked the DNA marker, Lane 2 showing negative control (DNA nuclease free water), , lane 3- 7 marked positive cases showing amplified bands of 495 bp. (530 bp representing *GADPH* gene as positive control).

Amplification of mRNA- TGFβ1 gene by RT-PCR:

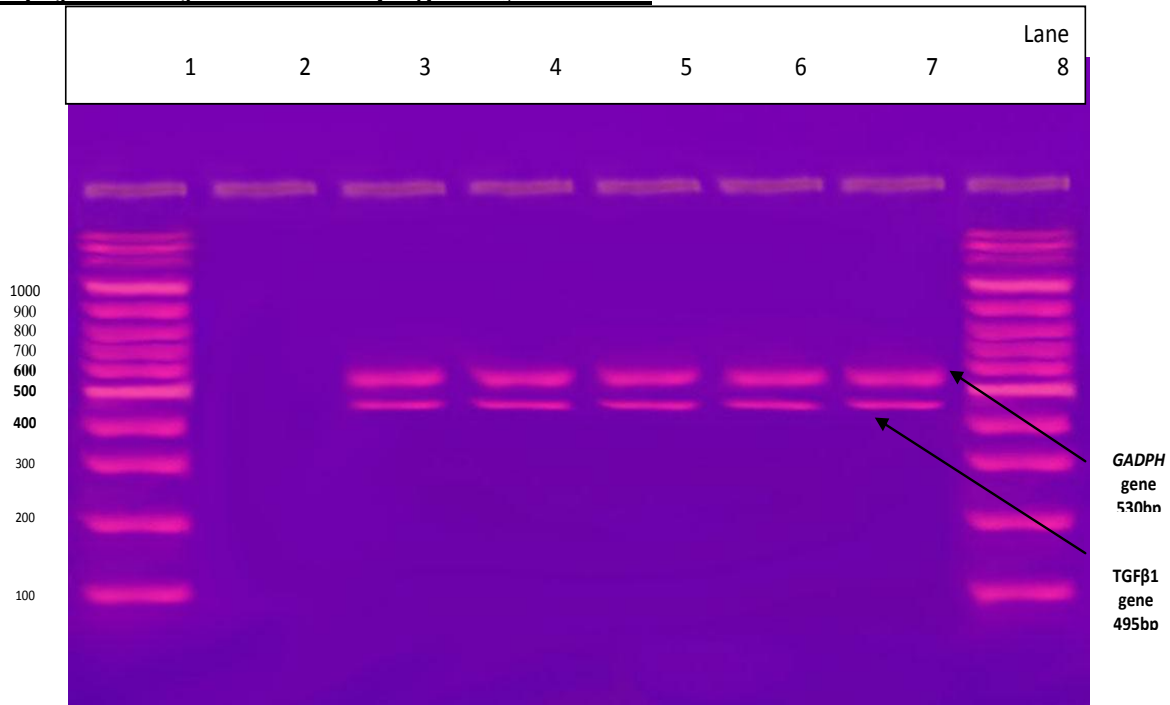


Figure (28): Ethidium bromide stained agarose gel showing bands of amplified PCR products of *mRNA- TGFβ1* gene of Sub of group B – 3i: 5 mice were treated by shark care drug dissolved in drinking water daily for 21 days blood samples: Lane 1 and 8 marked the DNA marker, Lane 2 showing negative control (DNA nuclease free water), , lane 3- 7 marked positive cases showing amplified bands of 495 bp. (530 bp representing *GADPH* gene as positive control).

Amplification of mRNA- *TGFβ1* gene by RT-PCR:

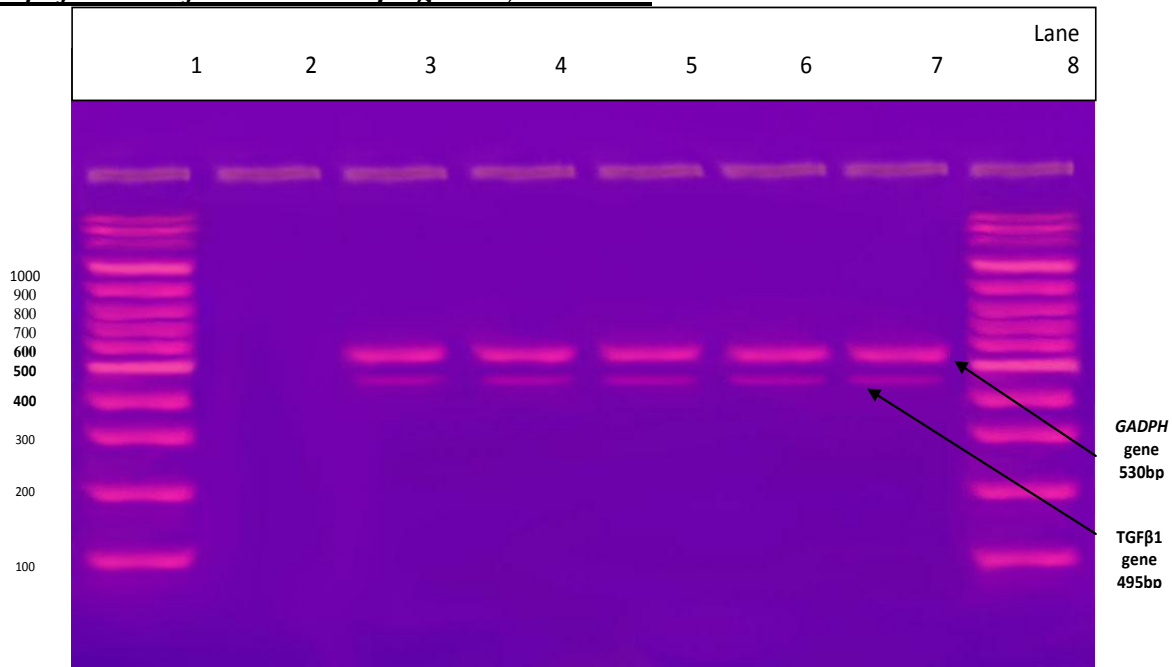


Figure (29): Ethidium bromide stained agarose gel showing bands of amplified PCR products of *mRNA- TGFβ1* gene of Sub of group B – 3ii: 5 mice were treated by shark care drug dissolved in drinking water daily for 21 days and were exposed to(LG1100) MCP corp for 5 sec blood samples: Lane 1 and 8 marked the DNA marker, Lane 2 showing negative control (DNA nuclease free water), , lane 3- 7 marked positive cases showing amplified bands of 495 bp. (530 bp representing *GADPH* gene as positive control).

Amplification of mRNA- *TGFβ1* gene by RT-PCR:

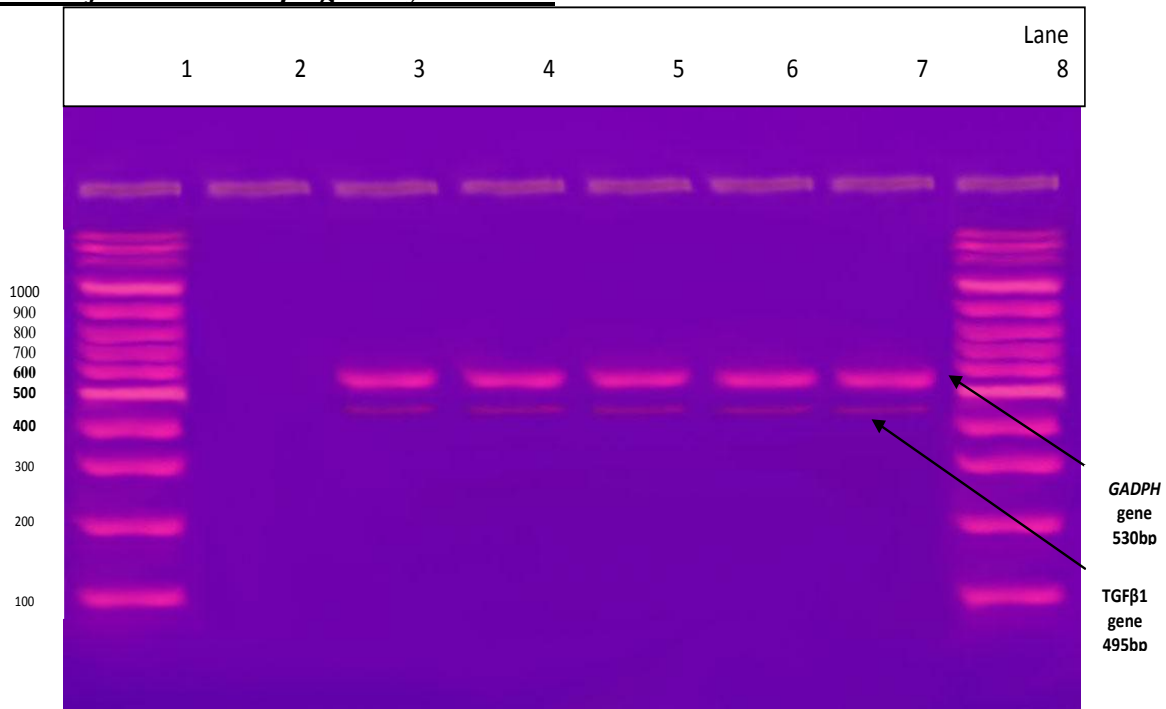


Figure (30): Ethidium bromide stained agarose gel showing bands of amplified PCR products of *mRNA- TGFβ1* gene of Sub of group B – 3iii: 5 mice were treated by shark care drug dissolved in drinking water daily for 21 days and were exposed to(LG1100) MCP corp for 10 sec blood samples: Lane 1 and 8 marked the DNA marker, Lane 2 showing negative control (DNA nuclease free water), , lane 3- 7 marked positive cases showing amplified bands of 495 bp. (530 bp representing *GADPH* gene as positive control).

The effects of pulsed electric fields on biological cells and tissues have been the topic of research for many years. The earliest report of bioeffects arising from the direct application of voltage using contact techniques (as opposed to contactless exposure using electromagnetic radiation) was when Stampfli and Willi reported on electric induced changes of cell membranes in 1957. In particular they measured changes in membrane conductivity and membrane potential. They further found that membrane damage is irreversible if the applied electric pulses are longer but otherwise the membrane is restored to its original characteristic. Almost a decade later, damaging effects of strong electric field on bacteria were reported suggesting nonthermal membrane interactions. Subsequent experiments showed that strong electric field pulses caused the increase in permeability of the plasma membrane of a biological cell.⁽¹⁷⁾

The relative high control value of cell membrane permittivity (ϵ) and conductivity (σ) may be attributed to the high value of the membrane capacitance and conductance due to normal value of cell membrane potential and distribution of ions dipoles. So the low values of the membrane permittivity and conductivity may be due to the lipid peroxidation, which causes cell membrane damage, cell death.⁽¹⁷⁾

Decreasing in the real permittivity for the group treated by 5-Fluorouracil as the time increase indicates that the degree of hepatic healing or therapy seem to be time – dependent the increasing in the real permittivity for the group treated by shark care for 5 sec in comparison with the same group treated with 5-Fluorouracil may be resulted from a rise in membrane capacitance due to the increase in membrane surface resulting from cell swelling.⁽¹⁸⁾

Beebe and coworkers first showed that applying ultrashort, pulsed electric fields (PEF) to mammalian cells and solid tumors results in reduced tumor growth, and induction of apoptosis in the treated cells.^(19,20) A number of studies have confirmed these observations, showing that PEFs do induce apoptosis in a number of cancer cell type in vitro and tumors in vivo.

The proposals of using pulsed electric fields to pursue the treatment of cancer free of cytotoxic

drugs and to achieve selective killing of tumor cells by inducing apoptosis is worthwhile to examine. Many cancers were resistant to current treatments and there was an urgent need for therapeutic innovations and discovery. There were currently three pulsed electric field therapies being tested on various tumor types in animals and preclinical studies. The aim of these minimally invasive treatments was to limit surgery and reduce side effects, scarring, pain, and mortality of patients while remaining cost-effective and safe. This review provides a brief overview of these therapies and their current stage in clinical research.

Tissue is a high in homogenous material it is obvious that interfacial processes play an important role in the electrical properties of tissue. This can be explained from figures (7-16) which illustrated the variation of permittivities and conductivities of the treated either by 5-Fluorouracil for 5 and 10 sec or by shark care for 5,10 sec respectively. The high permittivity values of the HCC mice group treated either by 5-Fluorouracil or shark care at low frequency level are correlated with Fricke & Morse⁽²¹⁾ and these can be attributed to change in cellular water content the amount of extra-cellular fluid, membrane properties, to change in the orientation of the malignant cells.

The cell plasma membrane consists of lipid bilayer with a thickness of approximately 5 nm. Its function is to protect the cell interior but also to facilitate the flow of selected types of ions and other materials from and to its surroundings. Under physiological conditions, the plasma membrane is subjected to a voltage difference caused by a system of ion pumps and channels in the membrane. Bioelectric fields are present whenever there is a potential difference between two regions in an organism. Every cell in our body generates this electric potential difference across the plasma membrane termed the resulting transmembrane voltage that is about 70 mv, inside negative.⁽²²⁾ In biophysics, cell membrane represent nonconducting, dielectric barriers and function as a near-ideal capacitor that can easily be charged by applying an external voltage pulse.⁽²³⁾ Consequently, large localized electric field

can be created across membranes that can then drive a host of bioeffects.

The exposure of a cell to an externally applied electric field results in an additional component of the voltage across the membrane.⁽²⁴⁾ This component, termed the induced transmembrane voltage, is superimposed onto the resulting voltage and exists only as long as the external field was present. With the accumulation of ions along the cell membrane, the potential difference across the membrane increases and the electric field inside the cell is reduced simultaneously.⁽²⁵⁾ The induced transmembrane voltage is proportional to the strength of the external electric field, and exposures to sufficiently strong fields can lead to transmembrane voltages far exceeding their physiological range.⁽²⁶⁾ Such large electric fields will exert a force on charged molecules such as water dipoles and can drive water into the lipid membrane to form a water-field defect or pore through the bilayer.⁽²⁷⁾ Such pores will allow the movement of small molecules across the membrane. This phenomenon was termed electroporation, or electropermeabilization.⁽²⁸⁻³⁰⁾ The possibility of curing electric pulses in cancer therapy may also rely on the different responses between cancers cells and normal cells. Cancer cells would have a higher apoptosis percentage than normal cells when exposed to the same electric field.⁽³¹⁾ And this finding are in agreements with our work that is to say that with increasing the time of the exposure to electric field the values of the permittivity show the higher value than it corresponding value at the same frequency.

The electric fields that are required to achieve cell death depend on the duration of the applied pulse, since this process involves the gradual changing of the capacitive sheath followed by the molecular rearrangement of the lipids.⁽³²⁾ These parameters of electric pulses play major roles in the type of effect on targeted cells. The PEF-based techniques creating irreversible cellular damage are divided in accordance to the pulse length hereafter. Their medical translations into cancer therapies are named irreversible electroporation (IRE).

Electrochemotherapy uses conventional electroporation with electric field durations in the

micro- to millisecond range this causes transient defects in plasma membrane, allowing the entry of poorly permeable drugs such as bleomycin to ablate tumors. Experimentally, the parameters that mainly influence the size of the ablated zone were the pulse amplitude, pulse duration, number of pulses, and to a lesser extent pulse repetition frequency of pulses. By modulating the parameters of the pulses as suggested by Davalos and coworkers it is possible to obtain a transmembrane potential high enough to ensure permanent permeabilization.⁽³³⁾ It has been found that the shorter the pulses, the higher the field strength necessary to observe the biological effects.⁽³⁴⁾ When a voltage gradient is applied long enough to a cell, charges accumulate at the plasma membrane creating an electric gradient across the membrane this transmembrane potential depends on the electric field amplitude. The most optimal parameters are being determined in vivo research and many differ per cancer type. For instance, 40 KV/cm electric pulses have been used to treat melanomas⁽³⁵⁾ or 35,50 and 68 KV/cm to treat hepatocellular cancer.⁽³⁶⁾

The larger the pulse number and the electric field, the larger will be the permeability increase in the plasma membrane.⁽³⁷⁾ Plasma membrane permeabilization may not be the only primary bioeffect of electric pulses. A number of studies by Chen and Co-authors indicated that electric pulses of supra-physiological voltage could cause damage to voltage gated (VG) ion channels⁽³⁸⁻⁴⁰⁾ or maybe by inhibition of VG ion channels as suggested in a study by Nesin and colleagues.⁽⁴¹⁾ Phosphatidylserine externalization inducing induction of apoptosis has been observed as well. Such result indicated the importance of the electric field in enhancing the effect of the chemotherapeutic agent (5-FU) in our work.⁽⁴²⁾

HCC exhibits numerous molecular abnormalities, which may be involved in the process of HCC development and progression. Thus, it is important to identify accurate predictors of prognosis and a reasonable selection criterion that can be applied to patients with HCC, particularly with early stage HCC, for rational treatment decisions remains a challenging task.⁽⁴³⁾ During the diagnosis of

HCC, a combination assay of at least two or three markers is recommended for a more sensitive and specific diagnosis of HCC. However, these traditional biomarkers do not reflect the biological features of the tumor or provide information about HCC behavior; thus, they do not allow the physician to accurately predict the outcomes of HCC patients. In the emerging era of new molecular targeted therapy for HCC, the evaluation of these novel agents will also require novel improvements in both the efficacy of the traditional biomarkers as well as other serological markers.

In the present study molecular study of AFP and TGF- β 1 gene expression as a molecular diagnostic and prognostic markers for HCC revealed a significant increase in the expression of AFP-mRNA and TGF- β 1-mRNA genes at sub group B1 after administration of DAB as compared to group A, at the same time histopathological changes were also seen.

The data in the present study showed that during the whole course of experiment the histopathological changes were synchronized with the biochemical changes. According to current results, there were an agreement with other studies done by several authors. ⁽⁴³⁻⁵⁰⁾ Finally our study further support that molecular detection of AFP-mRNA and TGF- β 1-mRNA genes expression using RT-PCR could be used as a diagnostic and prognostic predictor of HCC.

Conclusion

From the present study it could be suggested that therapeutic effect of shark care drug showed promising results for treatment of HCC compared to results obtained with 5-Fluorouracil drug. presence of electric field results in reduced tumor growth, and induction of apoptosis in the treated cells by enhancing uptake of chemotherapy and delivering anticancer drugs with enhanced efficacy and fewer adverse effects.

Recommendation

From the present study it could be recommended that use of shark care drug for treatment of HCC with increasing duration of

treatment course. Also use of electric field for enhancing uptake of chemotherapy and delivering anticancer drugs with enhanced efficacy and fewer adverse effects.

References

1. Bosch FX, Ribes J, Cleries R, Diaz M. Epidemiology of hepatocellular carcinoma. *Clin Liver Dis* (2005); 9: 191-211. DOI: [10.1016/j.cld.2004.12.009](https://doi.org/10.1016/j.cld.2004.12.009)
2. Yu MC, Yuan JM, Govindarajan S, Ross RK. Epidemiology of hepatocellular carcinoma. *Can J Gastroenterol* (2000); 14:703-9.
3. Lim SO, Park SJ, Kim W, Park SG, Kim HJ, Kim YI, et al. Proteome analysis of hepatocellular carcinoma. *Biochem Biophys Res Commun* (2002); 291(4):1031-7. DOI: [10.1006/bbrc.2002.6547](https://doi.org/10.1006/bbrc.2002.6547)
4. Reynolds JE. Martindale the Extra Pharmacopoeia. 31st ed. The Royal Pharmaceutical Society, London(1996).
5. Berndtsson M, Hagg M, Panaretakis T, Havelka AM, Shoshan MC, Linder S. Acute Apoptosis by cisplatin requires induction of reactive oxygen species but is not associated with damage to nuclear DNA. *Int J Cancer* (2007); 120(1):175-80. DOI: [10.1002/ijc.22132](https://doi.org/10.1002/ijc.22132)
6. Mookerjee A, Basu JM, Majumder S, Chatterjee S, Panda GS, Dutta P, et al. A novel copper complex induces ROS generation in doxorubicin resistant Ehrlich ascitis carcinoma cells and increases activity of antioxidant enzymes in vital organs in vivo. *BMC Cancer* (2006); 6:267-78. DOI: [10.1186/1471-2407-6-267](https://doi.org/10.1186/1471-2407-6-267)
7. Tuorkey MJ, Abdul-Aziz KK. A pioneer study on the anti-ulcer activities of copper nicotinate complex [CuCl(HNA)₂] in experimental gastric ulcer induced by aspirinpyloris ligation model(Shay model). *Biomed Pharmacother* (2009); 63(3):194-201. DOI: [10.1016/j.biopha.2008.01.015](https://doi.org/10.1016/j.biopha.2008.01.015)
8. El-Saadani MA. A combination therapy with copper nicotinate complex reduces the adverse effects of 5-fluorouracil on patients

- with hepatocellular carcinoma. *J Exp Ther Oncol* (2004); 4(1):19-24.
9. Benet LZ, Kroetz DL, Sheiner LB: Pharmacokinetics: the dynamics of drug absorption, distribution, and elimination. In: Hardman JG, Limbird LE, Molinoff PB, Ruddon RW, ed. *Goodman & Gilman's the pharmacological Basis of Therapeutics*, 9th ed.. New York: McGraw-Hill; (1996), pp. 3-27.
 10. Uzzan B, Nicolas P, Cucherat M, Perret G. Microvessel Density as a prognostic Factor in Women with breast cancer: A systematic Review of the Literature and Meta-Analysis. *Cancer Research* (2004); 64: 2941-55. DOI: [10.1158/0008-5472.CAN-03-1957](https://doi.org/10.1158/0008-5472.CAN-03-1957)
 11. Lewis JV. *Illustrated Guide to Diagnostic Tests: Student Version*. Springhouse, PA: Springhouse Corp (pub); (1994). P. 578-645.
 12. Gingras D, Renaud A, Mousseau N and Beliveau R, Shark cartilage extracts as antiangiogenic agents: Smart drinks or bitter pills? *Cancer Metast Rev* (2000); 19: 83-6. DOI: [10.1023/A:1026504500555](https://doi.org/10.1023/A:1026504500555)
 13. Li H, Forstermann U. Nitric oxide in the pathogenesis of vascular disease. *J Pathol*, (2000); 190:244-54. DOI: [10.1002/\(SICI\)1096-9896\(200002\)190:3<244::AID-PATH575>3.0.CO;2-8](https://doi.org/10.1002/(SICI)1096-9896(200002)190:3<244::AID-PATH575>3.0.CO;2-8)
 14. Polk, C. and Potow, E., "Handbook of Biological Effects of Electromagnetic Field". CRC Press, Inc. Tokyo (1996).
 15. Irimajiri, A, Asmi, K. and Kinoshita, Y., Passive electrical properties of the membrane and cytoplasm of cultured rat basophile leukaemia, *Biochimica et biophysica Acta* (1987); 86-203.
 16. Irimajiri, A, Asmi, K. and Kinoshita, Y., and Takashima, S., Dielectric properties of mouse lymphocytes and erythrocytes. *Biochimica et Biophysica Acta*.(1988); 1010:49.
 17. O'Shea JJ, Paul WE. Regulation of T(H)1 differentiation controlling the controllers *Nat Immunol* 2002;3(6):506-8. DOI: [10.1038/ni0602-506](https://doi.org/10.1038/ni0602-506)
 18. Hammerich D., Ozkan O.R., Tsai J-Z., Staelin S.T., Tungiitkusolmum S., Mahvi D.M., Webster J.G., Changes in electric resistivity of swine liver after occlusion and postmortem *Med. Biol. Eng. comput* 2002;40:29-33. DOI: [10.1007/BF02347692](https://doi.org/10.1007/BF02347692)
 19. Beebe SJ, Fox P, Rec LJ, Somers K, Stark RH, Schoenbach KH. Nanosecond pulsed electric field (nsPEF) effects on cells and tissues: Apoptosis induction and tumor growth inhibition. *IEEE Transactions on Plasma Science*. (2002); 30(1):286-92. DOI: [10.1109/TPS.2002.1003872](https://doi.org/10.1109/TPS.2002.1003872)
 20. Beebe SJ, White J, Blackmore PF, Deng Y, Somers K, Schoenbach KH. Diverse effects of nanosecond pulsed electric fields on cells and tissues. *DNA Cell Biol.*(2003);22:785-96. DOI: [10.1089/104454903322624993](https://doi.org/10.1089/104454903322624993)
 21. Frick H, and Morse S., the electric capacity of tumors of the breast. *J.cancer Res.*(1982); 20:422.
 22. Altunc S, Baum CE, Christodoulou CG, Schamiloglu E. Spatially Limited Exponential Lens Design for Better Focusing an Impulse. *Proc. URSI General Assembly*. August (2008), Chicago, IL.
 23. Joshi RP, Hu Q. Case for applying subnanosecond high-intensity, electrical pulses to biological cells. *IEEE Trans Biomed Eng.* (2011);58(10):2860-6. DOI: [10.1109/TBME.2011.2161478](https://doi.org/10.1109/TBME.2011.2161478)
 24. Schoenbach KH, Hargrave B, Joshi RP, Kolb JF, Osgood C, Nuccitelli R, Pakhomov A, Swanson RJ, Stacey M, White JA, Xiao S, Zhang J, Beebe SJ, Blackmore PF, Buescher ES. Bioelectric effects of intense nanosecond pulses. *IEEE Trans. Dielect. Electr. Insul.* (2007);14(5):1088-1119. DOI: [10.1109/TDEI.2007.4339468](https://doi.org/10.1109/TDEI.2007.4339468)
 25. Swanson RJ, Stacey M, White JA, Xiao S, Zhang J, Beebe SJ, Blackmore PF, Buescher ES. Bioelectric effects of intense nanosecond pulses. *IEEE Trans. Dielect. Electr. Insul.* (2007);14(5):1088-1119. DOI: [10.1109/TDEI.2007.4339468](https://doi.org/10.1109/TDEI.2007.4339468)
 26. Joshi RP, Song J, Schoenbach KH, Sridhara V. Aspects of lipid membrane bio-responses to subnanosecond, ultrahigh voltage pulsing. *IEEE Trans. Dielectr Electr Insul* (2009);16(5):1243-50. DOI: [10.1109/TDEI.2009.5293934](https://doi.org/10.1109/TDEI.2009.5293934)
 27. Joshi RP, Song J, Schoenbach KH, Sridhara V. Aspects of lipid membrane bio-responses to subnanosecond, ultrahigh voltage pulsing. *IEEE Trans. Dielectr Electr Insul*

- (2009);16(5):1243-50. DOI: [10.1109/TDEI.2009.5293934](https://doi.org/10.1109/TDEI.2009.5293934)
28. Delemotte L, Tarek M. Molecular dynamics simulations of lipid membrane electroporation. *J Membr Biol* (2012);245:531-43. DOI: [10.1007/s00232-012-9434-6](https://doi.org/10.1007/s00232-012-9434-6)
 29. Neumann E, Rosenheck K. Permeability changes induced by electric impulses in vesicular membranes. *J Membr Biol*. (1972);10:279-90. DOI: [10.1007/BF01867861](https://doi.org/10.1007/BF01867861)
 30. Teissié J, Golzio M, Rols MP. Mechanisms of cell membrane electroporation: a minireview of our present (lack of?) knowledge. *Biochim Biophys Acta* (2005);1724:270-80. DOI: [10.1016/j.bbagen.2005.05.006](https://doi.org/10.1016/j.bbagen.2005.05.006)
 31. Escoffre JM, Portet T, Wasungu L, Teissié J, Dean D, Rols MP. What is (still not) known of the mechanism by which electroporation mediates gene transfer and expression in cells and tissues. *Mol Biotechnol* (2009);41:286-95. DOI: [10.1007/s12033-008-9121-0](https://doi.org/10.1007/s12033-008-9121-0)
 32. Tang LL, Sun C, Liu H, Mi Y, Yao CG, Li CX. Steep pulsed electric fields modulate cell apoptosis through the change of intracellular calcium concentration. *Colloids Surf. B Biointerfaces* (2007);57:209-14. DOI: [10.1016/j.colsurfb.2007.02.008](https://doi.org/10.1016/j.colsurfb.2007.02.008)
 33. Joshi RP, Schoenbach KH. Bioelectric effects of intense ultrashort pulses. *Crit Rev Biomed Eng.* (2010);38:255-304. DOI: [10.1615/CritRevBiomedEng.v38.i3.20](https://doi.org/10.1615/CritRevBiomedEng.v38.i3.20)
 34. Davalos R, Mir L, Rubinsky B. Tissue ablation with irreversible electroporation. *Ann Biomed Eng.* (2005);33:223-31. DOI: [10.1007/s10439-005-8981-8](https://doi.org/10.1007/s10439-005-8981-8)
 35. Breton M, Mir LM. Microsecond and nanosecond electric pulses in cancer treatments. *Bioelectromagnetics.* (2011) Aug 3. doi: [10.1002/bem.20692](https://doi.org/10.1002/bem.20692). DOI: [10.1002/bem.20692](https://doi.org/10.1002/bem.20692)
 36. Nuccitelli R, Chen X, Pakhomov AG, Baldwin WH, Sheikh S, Pomictier JL, Ren W, Osgood C, Swanson RJ, Kolb JF, Beebe SJ, Schoenbach KH. A new pulsed electric field therapy for melanoma disrupts the tumor's blood supply and causes complete remission without recurrence. *Int J Cancer.* (2009);125:438-45. DOI: [10.1002/ijc.24345](https://doi.org/10.1002/ijc.24345)
 37. Beebe SJ, Chen X, Liu JA, Schoenbach KH. Nanosecond pulsed electric field ablation of hepatocellular carcinoma. *Conf Proc IEEE Eng Med Biol Soc.* (2011);2011:6861-5. DOI: [10.1109/iembs.2011.6091692](https://doi.org/10.1109/iembs.2011.6091692)
 38. Frey W, White JA, Price RO, Blackmore PF, Joshi RP, Nuccitelli R, Beebe SJ, Schoenbach KH, Kolb JF. Plasma membrane voltage changes during nanosecond pulsed electric field exposure. *J Biophys* (2006);90:3608-15. DOI: [10.1529/biophysj.105.072777](https://doi.org/10.1529/biophysj.105.072777)
 39. Chen W, Lee RC. Evidence for electrical shock-induced conformational damage of voltage-gated ionic channels. *Ann NY Acad Sci* (1994);720:124-35. DOI: [10.1111/j.1749-6632.1994.tb30440.x](https://doi.org/10.1111/j.1749-6632.1994.tb30440.x)
 40. Chen W. Electroconformational denaturation of membrane proteins. *Ann NY Acad Sci.* (2005);1066:92-105. DOI: [10.1196/annals.1363.028](https://doi.org/10.1196/annals.1363.028)
 41. Chen W, Zhongsheng Z, Lee RC. Supramembrane potential induced electroconformational changes in sodium channel proteins: A potential mechanism involved in electric injury. *Burns* (2006);32:52-9. DOI: [10.1016/j.burns.2005.08.008](https://doi.org/10.1016/j.burns.2005.08.008)
 42. Nesin V, Bowman AM, Xiao S, Pakhomov AG. Cell permeabilization and inhibition of voltage-gated Ca²⁺ and Na⁺ channel currents by nanosecond pulsed electric field. *Bioelectromagnetics.* (2012);33:394-404. DOI: [10.1002/bem.21696](https://doi.org/10.1002/bem.21696)
 43. Vernier PT, Sun Y, Marcu L, Craft CM, Gundersen MA. Nanoelectropulse-induced phosphatidylserine translocation. *J Biophys* (2004)86:4040-80. DOI: [10.1529/biophysj.103.037945](https://doi.org/10.1529/biophysj.103.037945)
 44. Budhu A, Jia HL, Forgues M, Liu CG, Goldstein D, et al. Identification of metastasis related microRNAs in hepatocellular carcinoma. *Hepatology* (2008);47: 897-907. DOI: [10.1002/hep.22160](https://doi.org/10.1002/hep.22160)
 45. Zhou L, Liu J, Luo F. Serum tumor markers for detection of hepatocellular carcinoma. *World J Gastroenterol* (2006);12:1175-81.
 46. Li MS, Ma QL, Chen Q, Liu XH, Li PF, Du GG, et al. Alpha-fetoprotein triggers

- hepatoma cells escaping from immune surveillance through altering the expression of Fas/FasL and tumor necrosis factor related apoptosis-inducing ligand and its receptor of lymphocytes and liver cancer cells. *World J Gastroenterol* (2005);11:2564-9. DOI: [10.3748/wjg.v11.i17.2564](https://doi.org/10.3748/wjg.v11.i17.2564)
47. Cavin LG, Venkatraman M, Factor VM, Kaur S, Schroeder I, Mercurio F, et al. Regulation of alpha-fetoprotein by nuclear factor-kappaB protects hepatocytes from tumor necrosis factor-alpha cytotoxicity during fetal liver development and hepatic oncogenesis. *Cancer Res* (2004);64: 7030-8. DOI: [10.1158/0008-5472.CAN-04-1647](https://doi.org/10.1158/0008-5472.CAN-04-1647)
48. Belayew A, Tilghman SM. Genetic analysis of alpha-fetoprotein synthesis in mice. *Mol Cell Biol* (1982);2:1427-35.
49. Tilghman SM, Belayew A. Transcriptional control of the murine albumin/alpha-fetoprotein locus during development. *Proc Natl Acad Sci USA* (1982);79:5254-7. DOI: [10.1073/pnas.79.17.5254](https://doi.org/10.1073/pnas.79.17.5254)
50. Dong ZZ, Yao DF, Yao M, Qiu LW, Zong L, Wu W, et al. Clinical impact of plasma TGF-beta1 and circulating TGF-beta1 mRNA in diagnosis of hepatocellular carcinoma. *Hepatobiliary Pancreat Dis Int* (2008);7:288-95.
51. Derynck R, Goeddel DV, Ullrich A, Gutterman JU, Williams RD, Bringman TS, et al. Synthesis of messenger RNAs for transforming growth factors alpha and beta and the epidermal growth factor receptor by human tumors. *Cancer Res* (1987);47:707-12.